Highly sensitive quantitative and rapid immunochromatographic diagnosis of the clinical samples using scanning electron microscopy - preparing for future outbreaks.

Hideya Kawasaki*[a], Hiromi Suzuki[a], Masato Maekawa[b], Takahiko Hariyama*[a]

[a] Institute for NanoSuit Research, Preeminent Medical Photonics Education & Research Center, Hamamatsu University School of Medicine**,** Hamamatsu, Japan

[b] Department of Laboratory Medicine, Hamamatsu University School of Medicine, Hamamatsu, Japan

* Corresponding authors: Hideya Kawasaki, Takahiko Hariyama

Email: gloria@hama-med.ac.jp, hariyama@hama-med.ac.jp

ORCID account: 0000-0001-8923-7722, 0000-0001-9623-1011

Classification

Major: Biological sciences; Minor: Medical Sciences

Keywords: NanoSuit®; immunochromatography; infection detection; scanning electron microscopy; diagnostic test

Author Contributions: H.K. designed research; H.K., H.S., performed research; H.K. M.M., analyzed data; and H.K., T.H. wrote the paper.

The authors declare no competing interests.

Abstract

As pathogens such as the influenza virus and severe acute respiratory syndrome coronavirus 2 (SARS-CoV-2) can easily cause pandemics, the development of rapid diagnostic tests is crucial for implementing efficient quarantine measures, providing effective treatments to patients, and preventing or containing a pandemic infection. Here, we developed the immunochromatography-NanoSuit® method, an improved immunochromatography method combined with a conventional scanning electron microscope (SEM), which enables the observation of immunocomplexes labeled with a colloidal metal. The detection ability of our method is comparable to that of real-time reverse transcription-polymerase chain reaction and the detection time is within approximately 15 min. Our new immunochromatography-NanoSuit® method suppresses cellulose deformity and makes it possible to easily focus and acquire high-resolution images of

gold/platinum labeled immunocomplexes of influenza A, without the need for conductive treatment as with a conventional SEM. This easy and highly sensitive quantitative analysis by immunochromatography can be utilized to diagnose various infections in such as human and livestock, and highly infectious diseases including SARS-CoV-2.

Introduction

Infections are important threats to humanity. The novel influenza A(H1N1)pdm09 was declared a pandemic in 2009 (1). The current 2020 SARS-CoV-2 pandemic has had a devastating impact on human health and the world economy. The following factors are crucial for reducing the effects of these infections: 1: delayed invasion of infection into the country because of border measures and quarantine, 2: early containment strategies, and 3: early diagnosis to enable appropriate treatment. Therefore, rapid diagnostic tests (RDTs) are crucial for disease prevention, treatment, and pandemic containment (2). Although real-time reverse transcription-polymerase chain reaction (rRT-PCR) is a sensitive method, it is time-consuming, costly, and requires special equipment, professional expertise, and high-quality samples. For point-of-care testing, immunochromatography is easier to perform and useful for prompt disease detection, but its sensitivity and specificity are lower than those of rRT-PCR. However, improved specificity has been achieved by using lateral flow

biosensors (LFBs) with micro- and nano-materials (3). Signal readouts based on color, electrochemical signals, magnetic properties, luminescent, and surface-enhanced Raman spectroscopy have been integrated with LFBs for quantification analyses (3, 4). Nevertheless, these nanoparticle sensing methods are indirect. Direct observation of metal nanoparticles by electron microscopy (EM) for clinical use has not been reported because of the complexity of sample preparation and conventional EM operation. We recently reported a method of evaluating multicellular organisms in a high vacuum of an EM by encasing them in a thin, vacuum-proof suit, the 'NanoSuit®'(5), which can impart conductivity on a wet sample to avoid electron charges. Here, we combined the NanoSuit® method with immunochromatography. The new immunochromatography-NanoSuit® method (INSM) suppresses cellulose deformity, which causes blurring of particle images, and enables easy focus and acquisition of high-resolution images without the need for conductive treatment (6) as with a conventional scanning EM (SEM). This technology is a highly sensitive diagnostic tool for several pathogenic infections or other diagnoses.

Results

To investigate the sensitivity and specificity of immunochromatography using the NanoSuit® method, an influenza diagnostic kit was prepared (**Fig. 1*A***). The virus antigen (Influenza A nucleoprotein (NP)) reacted with a gold/platinum

(Au/Pt) labeled antibody in the sample to generate colored lines, indicating the presence of the antigen of interest in the sample (**Fig. 1*B* top, middle**). After the reaction, NanoSuit® solution (100 μL) was added upstream of the test-line (**Fig. 1*B* middle**), forming a thin NanoSuit® liquid layer (pale blue) (**Fig. 1*B* bottom**). The kit was positioned on the sample stage in the sample chamber of the SEM as close and parallel as possible to the camera (**Fig. 1*C***). The observation position of the test-line and background area were determined at fixed distances from the control-line border. The number of Au/Pt particles at the test-line and background area were counted in 6 fields of view at ×1200 (**Fig. 1*D***). Without NanoSuit® treatment, swelling of the cellulose and residual liquid present due to electron beam energy were observed (**Fig. 1*E***). In contrast, following NanoSuit® treatment, the cellulose membrane showed little or no swelling (**Fig. 1*F, G***). Au/Pt particles (arrows) of the test-line were clearly visualized (**Fig. 1*H***) compared to the background areas of the cellulose membrane **(Fig. 1*G***). Another immunochromatography diagnosis kit for detecting IgM antibodies against SARS-CoV-2 from Kurabo Industries Ltd. (Osaka, Japan) was tested using the NanoSuit® method (**Fig. 1*I***). The cellulose membrane image without the immunocomplex was clearly visualized after NanoSuit® treatment (**Fig. 1*J***). Approximately 25-nm countable gold nanoparticles (GNPs) of the control-line were detected (**Fig. 1*K*).**

Diagnoses based on macroscopic, EM, and rRT-PCR results were compared using 197 influenza-suspected clinical samples. rRT-PCR for influenza A was performed using the same clinical pharyngeal swab samples used in immunochromatography. To examine the relationship between the influenza copy number and rRT-PCR threshold, serial dilutions were performed (**Fig. 2*A***). A calibration curve (**Fig. 2*B***) was drawn to determine the relationship between copy number and cycle threshold (Ct) (**Fig. 2*C***). In our assay system, Ct ≤ 38.0 was calculated to be ≥151.4 copies/reaction.

The EM diagnosis for influenza A showed 94% clinical sensitivity (29/31) (95% confidence interval [95%CI]: 78.58–99.21%), 100% clinical specificity (95%CI: 97.80–100%) (**Fig. 2*D***), and a strong correlation (kappa; 0.99) compared with rRT-PCR (15.0 ≤ Ct ≤ 38.0) (**Fig. 2*E***). In contrast, standard macroscopic diagnosis showed 81% clinical sensitivity (25/31) (95%CI: 62.53–92.55%), 100% clinical specificity (95%CI: 97.80–100%) (**Fig. 2*D***), and a strong correlation (kappa; 0.97) compared with rRT-PCR (15.0 ≤ Ct ≤ 38.0) (**Fig. 2*E***).

Discussion

RDTs show variable assay performance with sensitivities of 10–70%, and up to 90% specificity compared to standard rRT-PCR-based assays (7). Their sensitivity has been improved by employing europium nanoparticles, showing

82.59% sensitivity and 100% specificity to clinically evaluate influenza A (H1N1) (8). The use of silver amplification immunochromatography in influenza virus detection kits showed 91.2% sensitivity and 95.8% specificity (9). Moreover, the rapid fluorescent immunochromatographic test employing CdSe/CdS/ZnS quantum dots showed 93.75% clinical sensitivity and 100% clinical specificity (10). However, the potential toxic effects of cadmium-based quantum dots are controversial (11). INSM is safe and showed the highest sensitivities (94% clinical sensitivity, 100% clinical specificity) in this study.

The development of an automated GNP counting system to replace manual counting using deep learning is in progress. Furthermore, there is a great potential for the clinical application of using an automated inexpensive SEM for immunochromatography in combination with INSM for SEM. Among the commonly used micro/nano-particles in immunochromatography, colloidal GNP is the most widely used (3). GNP is safe and can be easily conjugated with biomolecules, which subsequently retain their biochemical activity. Therefore, developing new GNP-based LFBs may be easier and faster than developing micro/nano-materials and can also be adapted quickly for new emerging infections such as SARS-CoV-2 (12). INSM is applicable to all LFBs, particularly in emergency tests to evaluate troponin, brain natriuretic peptide, and procalcitonin as measured by immunochromatography.

Diagnosis using the INSM high sensitivity, as it allows for direct particle observation. This method can be used to promptly diagnose new emerging infections including livestock and trigger LFB innovation.

Materials and Methods

Immunochromatography kit

The ImunoAce® Flu kit (NP antigen detection), a human influenza commercial diagnosis kit, was purchased from TAUNS Laboratories, Inc. (Shizuoka, Japan). Au/Pt nanoparticles were utilized to visualize the positive lines. Clinical samples of Flu kit were provided from the hospital and stored in biosafety box at room temperature. The IgM detection immunochromatography kit against SARS-CoV-2 was obtained from Kurabo Industries Ltd, (Osaka, Japan).

One step Real-time RT-PCR (rRT-PCR) for influenza A

rRT-PCR for influenza A was performed as described previously report using Flu A universal primers (13). A Ct within 38.0 was considered to be positive according to the CDC protocol (14). The primer/probe set targeted the human RNase P gene and served as an internal control for human nucleic acid as described previously (15).

SEM image acquisition

The immunochromatography kit was covered with the modified NanoSuit® solution based on previously published components (5) (Nisshin EM Co., Ltd., Tokyo, Japan), placed first onto the wide stage of the specimen holder, and then in an Lv-SEM (TM4000Plus, Hitachi High-Technologies, Tokyo, Japan). Images were acquired using the backscattered electron detectors with 10 or 15 kV at 30 Pa.

Ethical statement

The study was approved by the Hamamatsu University School of Medicine ethical committee (No.19-134), and all methods were performed following relevant guidelines and regulations.

Diagnosis and Statistics

The EM diagnosis and the criteria for a positive test were defined as follows: particle numbers from 6 fields from the background area and test-line were statistically analyzed using the *t*-test. If there were more than 5 particles in one visual field average and a significant statistical difference ($P < 0.01$) was indicated by the *t*-test, the test was considered as positive. Statistical analysis using the *t*-test was performed in Excel software. Statistical analysis of the assay sensitivity and specificity with a 95% confidence interval (95% CI) was performed using the MedCalc statistical website.

Footnotes

To whom correspondence may be addressed: Email: gloria@hama-med.ac.jp or hariyama@hama-med.ac.jp

Acknowledgments

The authors are thankful to Noriko Aoki (TAUNS Laboratories, Inc.) for providing rRT-PCR data of Influenza A and to Takafumi Miwa and Takumi Tandou (Hitachi, Ltd. Research & Development Group Nano-process Research Department) for advising SEM usage. We also thank the clinical laboratory center of Hamamatsu University School of Medicine, University Hospital for providing influenza immunochromatography test strips after routine examinations. This work was supported by JST START (grant number 714 [to H.K.]), by JSPS KAKENHI (grant numbers JP17K08784 [to H.K.] and JP18H01869 [to T.H.]), and by AMED (grant number A508 [to H.K.]).

References

1. D. L. Swerdlow, L. Finelli, Preparation for Possible Sustained Transmission of 2019 Novel Coronavirus: Lessons From Previous Epidemics. *JAMA* **323**, 1129-1130 (2020).
2. R. R, A. Dalal, H. Mohan, M. Prasad, C. S. Pundir, Detection methods for influenza A H1N1 virus with special reference to biosensors: a review. *Biosci Rep* **40** (2020).
3. Y. Huang *et al.*, Lateral flow biosensors based on the use of micro- and nanomaterials: a review on recent developments. *Mikrochim Acta* **187**, 70 (2019).
4. A. E. Urusov, A. V. Zherdev, B. B. Dzantiev, Towards Lateral Flow Quantitative Assays: Detection Approaches. *Biosensors (Basel)* **9** (2019).
5. Y. Takaku *et al.*, A thin polymer membrane, nano-suit, enhancing survival across the continuum between air and high vacuum. *Proc Natl Acad Sci U S A* **110**, 7631-7635 (2013).
6. H. Kawasaki *et al.*, The NanoSuit method: a novel histological approach for examining paraffin sections in a nondestructive manner by correlative light and electron microscopy. *Lab Invest* **100**, 161-173 (2020).
7. S. V. Vemula *et al.*, Current Approaches for Diagnosis of Influenza Virus Infections in Humans. *Viruses* **8**, 96 (2016).
8. S. T. Yu *et al.*, Clinical evaluation of rapid fluorescent diagnostic immunochromatographic test for influenza A virus (H1N1). *Sci Rep* **8**, 13468 (2018).
9. K. Mitamura *et al.*, Clinical evaluation of highly sensitive silver amplification immunochromatography systems for rapid diagnosis of influenza. *J Virol Methods* **194**, 123-128 (2013).
10. A. V. T. Nguyen *et al.*, Sensitive detection of influenza a virus based on a CdSe/CdS/ZnS quantum dot-linked rapid fluorescent immunochromatographic test. *Biosens Bioelectron* **155**, 112090 (2020).
11. E. Oh *et al.*, Meta-analysis of cellular toxicity for cadmium-containing quantum dots. *Nat Nanotechnol* **11**, 479-486 (2016).
12. C. Sheridan, Fast, portable tests come online to curb coronavirus pandemic. *Nat Biotechnol* (2020).
13. F. de-Paris *et al.*, Optimization of one-step duplex real-time RT-PCR for detection of influenza and respiratory syncytial virus in nasopharyngeal aspirates. *J Virol Methods* **186**, 189-192 (2012).
14. C. f. D. C. a. P. I. Division (2014) CDC Human Influenza Virus Real-Time RT-PCR Diagnostic Panel (CDC Flu rRT-PCR Dx Panel).
15. WHO Collaborating Centre for Influenza, GA. (2009) CDC protocol of realtime RTPCR for influenza A (H1N1).

Figures

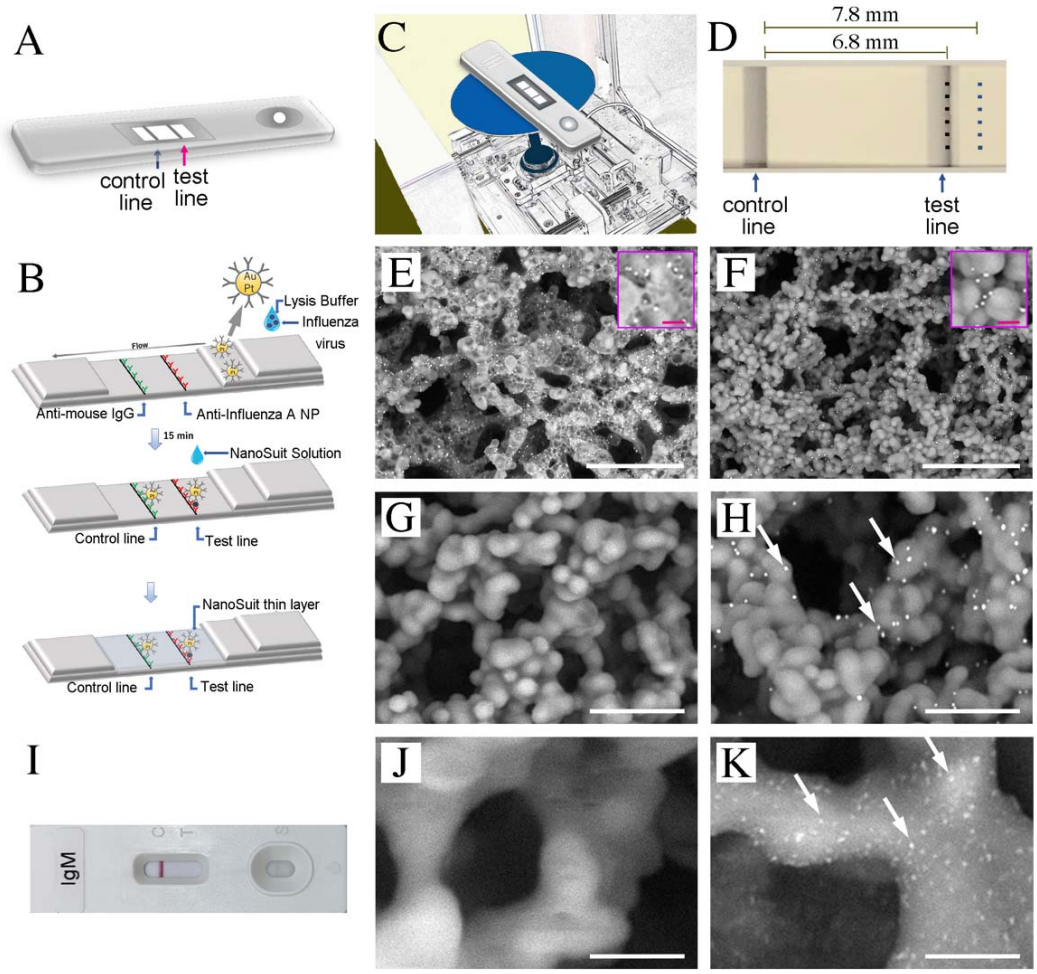

Figure 1. Sensitivity and specificity of immunochromatography using the NanoSuit® method. (***A***) Kit representation showing test and control lines. (***B***) Schematic diagram of the gold/platinum (Au/Pt)-Ab conjugate-linked rapid immunochromatographic kit. The immune-complex reacted with the anti-influenza A nucleoprotein (NP) at the test line and anti-mouse IgG at the control-line (top, middle). A NanoSuit® thin layer was formed after NanoSuit® treatment (bottom). (***C***) Kit placement in the SEM chamber. (***D***) Determination of the observation positions. Six fields were randomly selected in the test line and

background areas. (***E, F***) Images of cellulose and Au/Pt-labeled immunocomplex with immobilized antibody without (***E***) and with NanoSuit treatment (***F***). Scale bars in (***E***) and (***F***) = 15 μm. Inset is magnified image. Scale bars 600 nm. (***G***) Background image with NanoSuit® treatment. (***H***) Magnified image of (***F***). White arrows indicate the representative Au/Pt particles. Scale bars in (***G***) and (***H***) = 3 μm. (***I***) Immunochromatography diagnosis kit for IgM antibody against SARS-CoV-2. (***J***) Multiple gold nanoparticles (GNPs) (approximately 25-nm diameter) of the control-line on cellulose. White arrows indicate representative GNPs. (***K***) Background image. Scale bars in (***J***) and (***K***) = 600 nm.

A

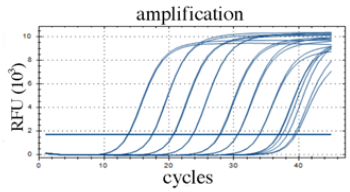

B

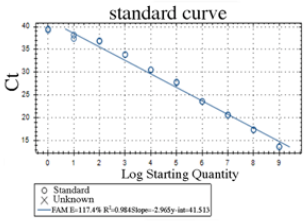

C

Sample (copies/μl)	Flu A Ct	
1.0×10^9	13.62	13.72
1.0×10^8	17.42	17.37
1.0×10^7	20.59	20.69
1.0×10^6	23.64	23.6
1.0×10^5	27.89	27.72
1.0×10^4	30.53	30.57
1.0×10^3	33.9	33.9
1.0×10^2	36.81	36.95
1.0×10^1	37.43	38.22
1.0×10^0	39.27	39.53

D

Influenza A rRT-PCR	Ct	Macroscopic diagnosis		Electron microscopic diagnosis	
		Sensitivity	Specificity	Sensitivity	Specificity
Positive (n=31)	15.0≤Ct<25.0	100% (10/10)		100% (10/10)	
	25.0≤Ct<30.0	92.8% (13/14)		100% (14/14)	
	30.0≤Ct≤38.0	28.5% (2/7)		71.4% (5/7)	
	15.0≤Ct≤38.0	80.6% (25/31)		93.5% (29/31)	
Negative (n=166)	Ct>38.0		100% (166/166)		100% (166/166)

E

		Macroscopic diagnosis			Electron microscopic diagnosis		
		positive	negative	Row Marginal	positive	negative	Row Marginal
Influenza A rRT-PCR	Positive	25	6	31	29	2	31
	Negative	0	166	166	0	166	166
Column Marginal		25	172	197	29	168	197
% Agreement(kappa)		0.97: 25+166/197			0.99: 29+166/197		

Figure 2. Comparison of macroscopic, electron microscopic (EM) and rRT-PCR influenza A diagnoses. (***A***) rRT-PCR amplification curve for influenza A. (***B***)

Standard curve for rRT-PCR of influenza A. (***C***) Relationship between cycle threshold (Ct) and sample copy numbers/reaction. (***D***) Clinical diagnostic performance of the EM assay. Thirty-one influenza A-rRT-PCR-positive samples were used to determine the sensitivity of the assays, and 166 influenza rRT-PCR-negative samples were used to determine the specificity of assays. (***E***) Comparison of EM diagnosis with rRT-PCR and macroscopic diagnosis of immunochromatography.

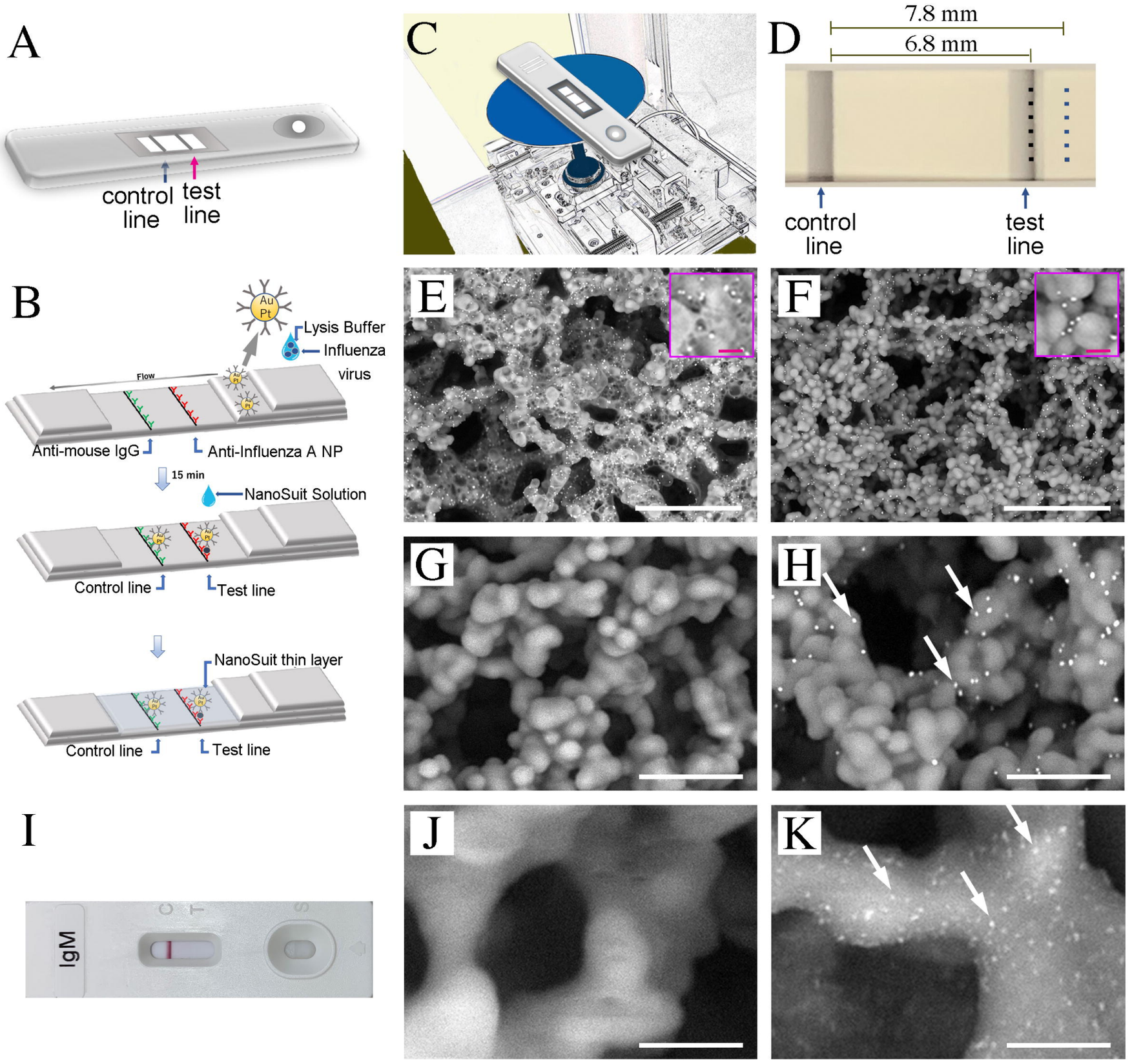
A
control line
test line
B
Au Pt
Lysis Buffer
Influenza virus
Flow
Anti-mouse IgG
Anti-Influenza A NP
15 min
NanoSuit Solution
Control line
Test line
NanoSuit thin layer
Control line
Test line
C
D
7.8 mm
6.8 mm
control line
test line
E
F
G
H
I
IgM
C
T
S
J
K

A

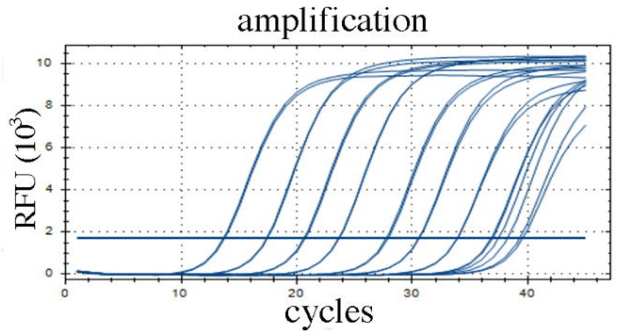

B

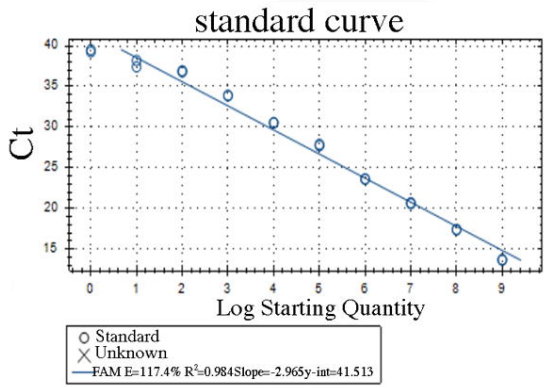

C

Sample (copies/μl)	Flu A Ct	
1.0×10^9	13.62	13.72
1.0×10^8	17.42	17.37
1.0×10^7	20.59	20.69
1.0×10^6	23.64	23.6
1.0×10^5	27.89	27.72
1.0×10^4	30.53	30.57
1.0×10^3	33.9	33.9
1.0×10^2	36.81	36.95
1.0×10^1	37.43	38.22
1.0×10^0	39.27	39.53

D

Influenza A rRT-PCR	Ct	Macroscopic diagnosis		Electron microscopic diagnosis	
		Sensitivity	Specificity	Sensitivity	Specificity
Positive (n=31)	15.0≤Ct<25.0	100% (10/10)		100% (10/10)	
	25.0≤Ct<30.0	92.8% (13/14)		100% (14/14)	
	30.0≤Ct≤38.0	28.5% (2/7)		71.4% (5/7)	
	15.0≤Ct≤38.0	80.6% (25/31)		93.5% (29/31)	
Negative (n=166)	Ct>38.0		100% (166/166)		100% (166/166)

E

		Macroscopic diagnosis			Electron microscopic diagnosis		
		positive	negative	Row Marginal	positive	negative	Row Marginal
Influenza A rRT-PCR	Positive	25	6	31	29	2	31
	Negative	0	166	166	0	166	166
Column Marginal		25	172	197	29	168	197
% Agreement(kappa)		0.97: 25+166/197			0.99: 29+166/197		